Uplift prior to continental breakup: Indication for removal of mantle lithosphere?

Raphael Esedo[1],*, Jolante van Wijk[1],*,†, David Coblentz[2],*, and Romain Meyer[3],*

[1]*Department of Earth and Atmospheric Sciences, University of Houston, 312 Science & Research Building 1, Houston, Texas 77204, USA*
[2]*Earth and Environmental Sciences Division, Los Alamos National Laboratory, MS D443, Los Alamos, New Mexico 87545, USA*
[3]*Centre for Geobiology and Department for Earth Science, University of Bergen, Allegaten 41, 5007 Bergen, Norway*

ABSTRACT

Uplift or reduced subsidence prior to continental breakup is a key component of the rift-drift transition. This uplift causes lateral variations in the lithospheric potential energy, which can increase intraplate deviatoric tension, thereby facilitating continental rupture. There is a growing body of evidence that pre-breakup uplift is a global phenomenon characteristic of magmatic and magma-poor rifted margins. Evidence is provided by the subaerial extrusion of lava interpreted from drill logs, stratigraphic records, the presence of breakup unconformities, and the spatial extent of uplift associated with Afar (the Ethiopian-Somali plateau), which may be at the stage of rupture. Previously discussed mechanisms contributing to this uplift include phase transitions, dynamic uplift from mantle plumes, and magmatic underplated bodies. We show in this study that dynamic uplift resulting from passive upwelling asthenosphere below the rift is limited (~200 m). Isostatic arguments suggest that removal of mantle lithosphere is a necessary and effective mechanism for uplift coincident with rupture. The combination of mantle phase transitions and a very thin mantle lid produces an excess potential energy state (as evidenced by a positive geoid anomaly) and leads to tensional forces favorable for rupture. These results underpin our proposed model for continental breakup where removal of mantle lithosphere by either detachment or formation of gravitational instabilities is a characteristic process. Observations of depth-dependent thinning and geochemical data support this model.

*Emails: Esedo: rcesedo@mail.uh.edu; van Wijk: jwvanwijk@uh.edu; Coblentz: coblentz@lanl.gov; Meyer: romain.meyer@geo.uib.no.
†Corresponding author.

INTRODUCTION

Passive margins are formed by horizontal extension of continental lithosphere that results in lithospheric thinning and subsequent subsidence or uplift to maintain isostatic balance. The stretching model of McKenzie (1978) provides a first-order estimate of the amount of tectonic subsidence associated with continental rifting (Fig. 1). When the crust and mantle lithosphere layers are thinned a relatively equal amount, subsidence of the surface and formation of a basin are expected. Uplift during extension is possible when the high-density mantle lithosphere thins relatively more than the crust (Fig. 1). During the continental rift phase, the surface usually subsides, and a comparison of the predicted basin subsidence and tectonic subsidence curves obtained from sediment layers generally gives good agreement (North Sea rift; McKenzie, 1978). For many rifted margins, however, the observed tectonic subsidence near the breakup axis is less than predicted. For example, subsidence curves of the Norwegian Vøring margin (e.g., Skogseid and Eldholm, 1989) show reduced subsidence of the margin and even uplift above sea level close to the continent-ocean boundary. Here, uplift initiated several million years before continental breakup, and normal subsidence resumed shortly after the onset of seafloor spreading. This finding is confirmed by the presence of subaerially erupted basalt flows (Menzies et al., 2002) drilled during the Integrated Ocean Drilling Program and Ocean Drilling Program on both conjugate margins of the northeastern Atlantic Ocean. Breakup elsewhere in the North Atlantic occurred at shallow-marine or subaerial conditions. Stratigraphic evidence and apatite fission track studies demonstrate latest Cretaceous–earliest Paleocene (i.e., just preceding rupture) uplift in East Greenland, around the British Isles, the Møre margin, and the Faeroe Shetland Basin (see Meyer et al., 2007, for an overview). There is also compelling evidence that the magma-
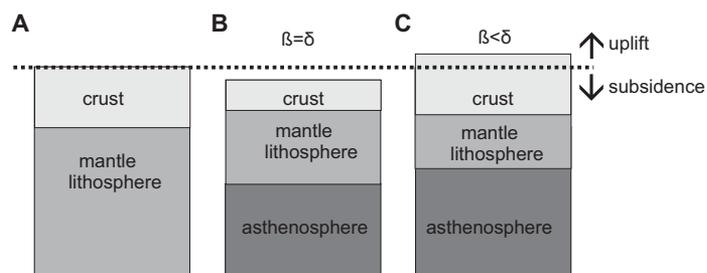

Figure 1. Isostatic balances show that surface uplift may result if the mantle lithosphere is proportionally thinned more than the crust during extension (McKenzie, 1978). β = crustal thinning, δ = mantle lithosphere thinning. (A) Reference column. Crust is 35 km thick with a density of 2800 kg/m^3, mantle lithosphere is 65 km thick with a density of 3300 kg/m^3, asthenosphere density is 3200 kg/m^3, water density is 1000 kg/m^3. (B) Thinning the crust and mantle lithosphere with a factor 2 ($\beta = \delta = 2$) results in ~1.7 km subsidence. (C) Approximately 1.3 km uplift is expected when $\beta = 1$ and $\delta = 3$.

poor Iberia-Newfoundland margin underwent reduced subsidence; sediments were deposited at shelf or outer shelf conditions instead of at 2–5 km depth around the time of breakup (Péron-Pinvidic and Manatschal, 2009).

Such uplift prior to breakup results in lateral variations in the lithospheric potential energy, which contributes to deviatoric tension within the plate. Although these stress changes are small compared to the extensional strength of the lithosphere, they can facilitate continental breakup (Sandiford and Coblentz, 1994). Buck (2006) found that the tectonic force required for rifting of normal thickness lithosphere is larger than available from plate tectonic forces in the absence of magmatic intrusions. Additional tensional forces associated with lithospheric potential energy variations produced during the pre-rupture uplift stage may provide the extra tensional stresses required for breakup.

In this study, we analyze the uplift history of rifted margins. There is strong evidence from the literature that uplift of rifts prior to continental breakup is a global phenomenon that occurs on both amagmatic and magmatic margins. Several mechanisms contribute to uplift during rifting, e.g., magmatic underplating, phase transitions, deep necking of the lithosphere, dynamic uplift, and loss of mantle lithospheric material, and they can contribute as much as several kilometers of uplift. We present results from numerical models that show that passive asthenospheric upwelling below a rift may also result in uplift, although the amount of dynamic topography is relatively small. Isostatic arguments for uplift during rifting suggest that the most effective uplift mechanism that results in an increase in the potential energy of the rift relative to the mean plate potential energy is thinning or loss of mantle lithosphere. Consequently, we propose that this mechanism is a normal process accompanying rupture.

UPLIFT OF RIFTS PRIOR TO SEAFLOOR SPREADING: OBSERVATIONS

A survey of rifted margins worldwide, including both magmatic and magma-starved margins, demonstrates that uplift (or at least reduced subsidence) prior to continental breakup is common (Table 1). On the magmatic margins of the North Atlantic Igneous Province, an uplift event before breakup in the latest Cretaceous–earliest Paleocene is well documented. Lava flows were deposited subaerially on the Norwegian margin (including the Møre and Vøring Basins), and there is evidence for influx of coarse sediment into the Møre Basin in response to regional exhumation and denudation of the mainland (Martinsen et al., 1999). A regional hiatus and erosion features are observed along the outer Vøring Basin (Skogseid et al., 1992). Stratigraphic evidence implies a similar subsidence pattern on the conjugate East Greenland margin (Larsen et al., 1999). In West Greenland, uplift of as much as 1.3 km prior to rupture was documented as having occurred 5–10 m.y. before the onset of volcanism. The uplift was associated with fluvial peneplanation, exhumation of deep-marine sediments, valley incision, and catastrophic deposition (Dam et al., 1998). Apatite fission track studies have identified an exhumation event in the late Cenozoic–Early Paleocene around the British Isles (Green et al., 2001). This uplift coincides with the Danian Maureen Formation deposition in the North Sea. Dynamic uplift by the Iceland mantle plume and magmatic underplating are the current explanations for the pre-rupture uplift in the northern North Atlantic (e.g., White and McKenzie, 1989). Farther south, several kilometers of uplift must have occurred on the magma-poor Iberia-Newfoundland margins, where Tithonian sediments were deposited at <~800 m depth, instead of at the expected 2–5 km depth (Péron-Pinvidic and Manatschal, 2009). This uplift has been explained by phase transitions in the mantle lithosphere (Simon and Podladchikov, 2008). The spinel-plagioclase transition in particular would be responsible for uplift of strongly extended lithosphere (Simon and Podladchikov, 2008). On the north Namibia magmatic margin uplift is inferred from the presence of a breakup unconformity (Gladczenko et al., 1997). The northern Gulf of Aden margin (Yemen) underwent a change from marine to fluvial to fluviolacustrine sediments, indicating uplift prior to breakup (Chazot et al., 1998). Further evidence for pre-breakup uplift of rifts is provided by the South China Sea margin, where Xie et al. (2006) found evidence of anomalous thermal subsidence, which they explained by a magmatic event.

The Afar region, where the Ethiopian rift part of the Red Sea–Gulf of Aden–East African rift system dissects the uplifted Ethiopian plateau, is currently at the point of continental breakup (Yirgu et al., 2006, and references therein). The magma-assisted rifting is thought to result in an evolving magmatic margin, although the long period of active volcanism is not typical for magmatic rifted margins. Volcanism started 45 Ma and continues today, giving rise to an igneous province ~1000 km wide covering Ethiopia and Yemen. The Afar depression has an elevation of ~200–1000 m above sea level. There is tomographic evidence for the presence of only a very thin mantle lithosphere below Afar (~15 km; Dugda et al., 2007). The current high elevation of the Afar region is attributed to dynamic support of the Afar mantle plume (Lithgow-Bertelloni and Silver, 1998).

Two periods of rifting are identified in the western Australian margin, Middle Jurassic and Neocomian (Falvey and Mutter, 1981), and they are marked by distinct breakup unconformities onshore. In the Perth Basin, formed during

TABLE 1. UPLIFT OF MAGMATIC AND AMAGMATIC MARGINS

Margin	Uplift and/or reduced subsidence evidence?	Rift-drift age	References
U.S. and Canada east coast (Carolina–Nova Scotia) (V)	Uplift of ~1.5–2 km interpreted from basin erosion	ca. 185–200 Ma	Withjack et al. (1998)
Namibia (V) and South America (V)	Uplift inferred from evidence of erosional rift unconformity and subaerial lava flows	Aptian	Gladczenko et al. (1997)
Galicia Bank, Iberia Abyssal Plane (NV)	Uplift inferred from stratigraphic evidence	Aptian	Peron-Pinvidic and Manatschal (2009), Wilson et al. (2001), Schärer et al. (2000)
Western Australia (V)	~1–2 km uplift and erosion of pre-break up sediments inferred from stratigraphy	Early Cretaceous	Song and Cawood (2000)
Eastern Australia (V)	~1–3 km of uplift from fission track evidence	ca. 95 Ma	Veevers (2000)
Norway and East Greenland (V)	Uplift inferred from drilled subaerial lava flows, fission track, and stratigraphy	ca. 54 Ma	Hjelstuen et al. (1999), Larsen et al. (1999), Meyer et al. (2007), Skogseid and Eldholm (1989)
West Greenland (V)	~1.3 km of sediments eroded; uplift interpreted from fluvial peneplanation, valley incision	Early-Late Paleocene	Dam et al. (1998)
Yemen (V)	Stratigraphy shows change from marine to fluvial to fluviolacustrine, Ethiopian-Yemen plateau uplifted ~ 1.6 km	ca. 35 Ma	Chazot et al. (1998), Yirgu et al. (2006)
South China Sea (NV)	Uplift inferred from evidence of breakup unconformity and tectonic subsidence analyses	ca. 30 Ma	Lin et al. (2003), Xie et al. (2006)
Afar (V)	Uplift ~1.6 km for Ethiopian plateau region	0 Ma	Yirgu et al. (2006)

Note: V—magmatic margin; NV—magma-poor margin.

the separation of India and Australia, breakup-related uplift has resulted in the erosion of pre-rift sedimentary sequences (Table 1). This uplift has been found to be greater in the offshore parts of the basin, where it is estimated that ~3200 m of pre-rift sediments have been removed. Both plume and non-plume models have been proposed to explain the rifting-related uplift in Western Australia (Mihut and Müller, 1998). The absence of substantial volcanism onshore and a lack of evidence of a hotspot track point toward a nonthermal explanation. The volcanic eastern and southeastern margins of Australia underwent uplift related to the 95 Ma breakup event, during which an estimated 1–3 km of section were eroded (Table 1). In southern Australia, a breakup unconformity is dated as 99 Ma, marking the separation from Antarctica. The uplift along this margin is interpreted to be due to underplating (Veevers, 2000; Song and Cawood, 2000).

Earlier studies (White et al., 1987) have pointed out that magmatic margins would largely remain close to sea level during rupture, while magma-starved margins would tend to subside by as much as 2 km. However, the compilation in Table 1, that includes more recent work, shows that amagmatic rifted margins undergo uplift as well. This body of evidence motivates us to revisit the role of uplift in continental rupture.

MECHANISMS FOR UPLIFT

Uplift of magma-dominated margins before the time of continental breakup has been explained by magmatic underplating and dynamic support of a mantle plume (e.g., White and McKenzie, 1989; Skogseid et al., 1992; Saunders et al., 1997). Magma that results from partial melting of warm plume material intrudes the lithosphere, and may freeze below the Moho or in the lower crust. The density of the frozen magma is estimated to be ~3000 kg/m^3, less than the density of continental mantle lithosphere, and therefore magmatic underplating results in permanent uplift (Skogseid and Eldholm, 1989). Isostatic balances show that this uplift is ~10% of the thickness of the underplated material (Maclennan and Lovell, 2002). The rising plume material is predicted to dynamically uplift the surface. When the rising diapir of hot mantle impinges on the base of the lithosphere, a domal uplift of between 500 and 1000 m is expected over an area ~600 km in diameter (Campbell, 2005). The high elevation of the Afar region has been explained by its proximity to the African superplume, and the Norwegian margins are thought to have been uplifted by the Iceland plume. This mechanism cannot explain the lat-erally elongated uplift pattern of the northern North Atlantic margins, or the uplift of magma-poor margins that are inferred to be formed outside the influence of mantle plumes or high-temperature mantle.

At magma-poor margins, uplift or reduced subsidence has been explained by phase transitions in the mantle during rifting. Phase transitions within the mantle lithosphere result from a temperature increase during rifting, and they affect material densities. Simon and Podladchikov (2008) determined the effects of mantle composition on lithospheric densities, and found that mantle garnet-spinel and the spinel-plagioclase transitions, especially, affect the density of the lithosphere during thinning. The lithospheric density reduction in the garnet-spinel transition during thinning may cause initial synrift uplift, while the density reduction in the spinel-plagioclase transition in highly extended areas may result in late synrift uplift (Simon and Podladchikov, 2008) or reduction of subsidence by ~1000 m.

The necking depth is defined as "the level of no vertical motion in the absence of gravitational forces" during stretching of the lithosphere (Keen and Dehler, 1997, p. 744). Tectonic isostatic studies (e.g., Braun and Beaumont, 1989; Kooi et al., 1992) suggest that if the depth of necking is within the crust, it gives rise ultimately to subsidence of the rift area. Such a shallow depth of necking implies that the crust is thinning proportionally more than the mantle lithosphere. In cases where the necking depth is subcrustal, and the mantle lithosphere thins proportionally more than the crust, the response is a regional flexural uplift. This mechanism could contribute to uplift of both magmatic and magma-poor margins. Geophysical data show that nonmagmatic margins such as the Iberia Abyssal Plain are characterized by strongly thinned crust, with crustal blocks separated by exhumed mantle lithosphere. This would be described as shallow necking, although considerable uplift occurred on this margin (Péron-Pinvidic and Manatschal, 2009).

Uplift during rifting may also result from upward flow beneath the rift (dynamic uplift) and from excessive thinning of continental mantle (Fig. 1). The uplift or subsidence as a result of depth-dependent thinning of continental lithosphere is calculated using an isostasy model (see Isostasy discussion). We use two-dimensional (2D) diagrams of crustal and mantle lithosphere thickness (called f_c/f_l diagrams, developed by Sandiford and Powell, 1990) in which the simultaneous isostatic effect of depth dependent crust and mantle thinning is analyzed. In the diagrams, uplift and subsidence paths show the effect of progressive depth-dependent thinning and phase transitions. Dynamic uplift during rifting is studied with upper mantle convection models (discussion following), as this uplift results from upper mantle flow induced by the rifting process.

Models of Dynamic Uplift

During rifting and lithosphere thinning, asthenosphere wells up below the rift zone, and this flow may exert a stress on the base of the lithosphere, driving dynamic uplift during rifting. Dynamic uplift or subsidence results from stresses imposed on the lithosphere by mantle flow. Large upwelling structures in the mantle may produce ~1.5 km dynamic topography (Conrad and Gurnis, 2003; Gurnis et al., 1998; Moucha et al., 2009), while small-scale convection in the upper mantle related to lithospheric instabilities may produce as much as ~100 m dynamic topography (Elkins-Tanton, 2005). Does upward mantle flow during rifting result in dynamic topography? We calculated dynamic topography during rifting using a geodynamic model of upper mantle flow. Asthenosphere upwelling during rifting was modeled using the finite element software package CitCom (Moresi and Gurnis, 1996; Zhong et al., 2000; van Hunen and Zhong, 2003). A 2D model was used, with a model domain that is 660 km deep and ~1500 km wide, divided into a visco-plastically deforming high-viscosity lithosphere overlying a viscous upper mantle. The visco-plastic lithosphere rheology combines linear temperature- and pressure-dependent viscous Arrhenius-type rheology for diffusion creep with a pseudoplastic rheology for Byerlee's law. More detailed descriptions of this model can be found in van Hunen and Zhong (2003) and van Wijk et al. (2008). We used the following rheological parameters: activation energy E* = 360 kJ/mol, and activation volume V* = 5 cm^3/mol. The reference viscosity (the viscosity at mantle temperature of 1350 °C and 660 km depth) was $\eta_0 = 1.76 \cdot 10^{22}$ Pa·s. Other parameters that were used include thermal expansion coefficient α = $3.5 \cdot 10^{-5}$ K^{-1}, diffusivity K = $1 \cdot 10^{-6}$ m^{2}s^{-1}, specific heat c_p = 1250 J · kg^{-1} · K^{-1}, density ρ = 3300 kg/m^3, and gravitational acceleration g = 9.8 m/s^2. These model parameter values were adopted from van Hunen and Zhong (2003); the activation energy and volume are from Karato and Wu (1993). Thermal boundary conditions are 0 °C at the free surface, 1350 °C at the bottom of the model domain, and zero diffusive heat flux at the side boundaries. Constant velocities are prescribed on the left and right sides of the model domain to extend the lithosphere. A small weak zone (with ~10% thinner lithosphere over an ~100-km-wide zone) is present

in the center of the domain to localize the formation of the rift zone.

In the model of extension, a rift zone is formed where the small weak zone was initially prescribed. Because we are only interested here in the resulting dynamic topography, one representative simulation (extension rate 16 mm/yr) is shown in Figure 2. Upon formation of the rift zone, the lithosphere thins and asthenosphere is emplaced at shallow depths. The upward flow of asthenosphere below the rift has a maximum vertical velocity of almost 30 cm/yr (indicated by the arrows in Fig. 2); this maximum amplitude is found late in the synrift stage and results in dynamic topography. Dynamic topography resulting from this upward flow is calculated from the stress exerted by mantle flow on the lithosphere. For calculating the dynamic topography, we used a time step where upward flow is maximum (shown in Fig. 2).

We find that a maximum dynamic uplift of ~200 m is predicted during the late synrift stage, centered around the rift axis; during the earlier rift phase the amplitude of the dynamic uplift is less. The dynamically uplifted zone is in this test ~300 km wide, and therefore also affects the margins of the rift or breakup zone. Simon and Podladchikov (2008) found that phase transitions may account for ~1000 m of uplift, and magmatic underplating may contribute an amount equal to ~10% of the thickness of the underplated body. Compared to these mechanisms, dynamic uplift resulting from upwelling asthenosphere below the rift is a relatively small contribution.

Isostasy

Depth-dependent thinning of the lithosphere affects the elevation of the rift zone at continental rupture. How the lithospheric thinning is partitioned between the crust and mantle lithosphere has an important impact on the surface displacement. For example, thinning of only the crust results in subsidence of the rift zone, while thinning of only the mantle lithosphere results in uplift during rifting (McKenzie, 1978; Fig. 1). Huismans and Beaumont (2011) showed that lithosphere thinning is likely highly differential. Here we analyze uplift and subsidence patterns during rifting using a lithospheric model in isostatic balance with variations in the crustal and mantle lithospheric strains. As many margins have undergone various rifting episodes, and estimates of crustal and mantle lithosphere thicknesses during and prior to rifting are not well constrained, only representative layer thicknesses will be considered here to calculate isostatic balances. Typically, models consider only the independent effects of changes to either the crust or mantle lithosphere without accounting for simultaneous modification of both components. It is the competing isostatic influences of both lithospheric elements that will dictate the magnitude of elevation changes. The f_c-f_l diagram (Sandiford and Powell, 1990; Coblentz and Stüwe, 2002) provides a convenient way to evaluate how vertical strains in the lithosphere may be decoupled between crustal and mantle components (Fig. 3). Following Sandiford and Powell (1990), we defined f_c as the ratio of deformed to referenced crustal thickness and f_l as the ratio of the deformed to reference total lithospheric thickness. Thus, the origin of
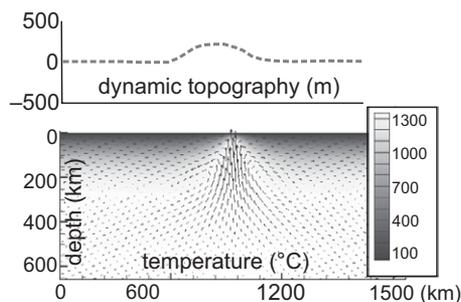

Figure 2. Dynamic uplift (upper panel) resulting from late synrift mantle flow (lower panel). Arrows are mantle flow lines, gray scale is temperature (in °C). Approximately 200 m maximum dynamic uplift is predicted centered on the rift.
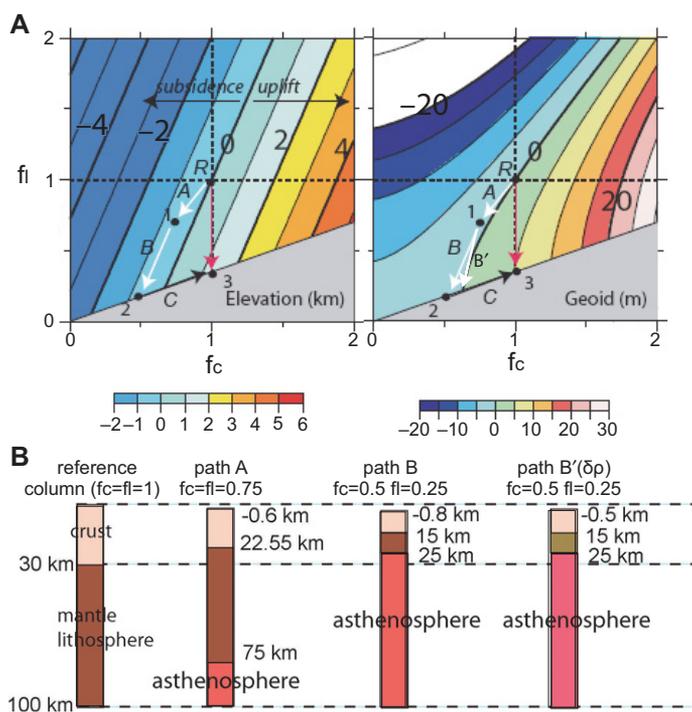

Figure 3. Isostatic diagrams to illustrate the effects of depth-dependent thinning and lithospheric modification on the isostatic response of the lithosphere, and predicted geoid anomalies; f_c **is crustal thinning,** f_l **is lithosphere thinning (calculated as percent strain). Values <1 indicate thinning. Units on the color bar are elevation (in km; left panel) and geoid (in m; right panel). Points 1, 2, and 3 are end points of the different paths. (A) Surface elevation changes in response to crustal and lithospheric thickness variations. Right panel: geoid anomaly (see Coblentz et al., 2011, and text for description of how this geoid is calculated). The arrows (paths) show the uplift and subsidence trends. R is the starting point (undisturbed lithosphere); the red arrow connects the starting and end points. (B) Isostatic columns corresponding to paths A, B, and B′. B′ is a modification of path B, including density variations due to phase transitions. In path B′ the density of the entire mantle lithosphere has been decreased by 2.3%. See text for further explanation.**

the f_c-f_l plane ($f_c = 0$, $f_l = 0$) corresponds to an undeformed equilibrium lithosphere, a state that the crust and lithosphere will tend toward in the absence of deformational forces. Here, we assume a reference lithospheric column represented by 30 km of 2800 kg/m^3 crust overlying mantle lithosphere with a density of 3300 kg/m^3 extending to a depth of 100 km. Density varies linearly as a function of temperature (and depth) in the column. Completely undeformed lithosphere is at the center of the f_c-f_l plane (Fig. 3) with larger and smaller values of f_c and f_l corresponding to thicker and thinner crustal or lithospheric thicknesses, respectively.

Thinning of the crust and/or mantle lithosphere during rifting produces a path in the f_c-f_l diagram indicating the amount of uplift or subsidence. Figure 3 illustrates the variations in surface elevation and geoid anomaly corresponding to variations in f_c and f_l values representing plausible crustal and mantle lithosphere configurations during rifting. In this analysis, the predicted geoid is based on the approach of Haxby and Turcotte (1978), which showed that in the limit of long wavelength and complete isostatic compensation, the geoid anomaly caused by density variations above the depth of compensation is proportional to the vertical dipole moment of the mass distribution above the depth of compensation:

$$\Delta N = \frac{2\pi G}{g} \int_S^D z \Delta\rho(z)\, dz, \qquad (1)$$

where ΔN is the geoid anomaly, G is Newton's gravitational constant, g is the value of gravitational acceleration on the reference ellipsoid, D is the depth of compensation (the depth below geoid at which pressure becomes equal beneath columns in isostatic balance, or here, where lateral density differences cease), S is the surface elevation, z is the depth, and $\Delta\rho(z)$ is the lateral difference in density from a reference lithosphere, including crust.

Three deformational paths (A, B, and C) are considered in Figure 3: path A corresponds to equal amounts of thinning of the crust and lithosphere. It begins at the reference state (the unextended state, point R). Path B delineates subsequent deformation where the lithosphere thins more than the crust. In this case, the predicted subsidence of the rift is less than expected if the direction of path A would have been continued. This is interpreted as reduced subsidence or relative uplift of the rift. The column B′ ($\delta\rho$) is a modification of path B that includes the effect of a mantle that has been modified by phase transitions, with resulting reduction in density (Simon and Podladchikov, 2008). In these calculations (B′) the entire mantle litho-

sphere column density has been modified; this is an upper limit as only a small part of the mantle lithosphere is normally expected to undergo a phase transition (Simon and Podladchikov, 2008). The reduction in density results in uplift (or reduced subsidence) of the rift. Path C represents the effect of subsequent crustal thickening. This could be a result of formation of lower crustal magmatic bodies. For simplicity, crustal density was not modified to calculate path C. In this case, the deformation results in absolute uplift of the rifted area and a positive geoid (and gravitational potential energy) anomaly. Lithospheric density variations (producing variations in the gravitational potential energy) result in long-wavelength lithospheric stresses (Coblentz and Sandiford, 1994). These tectonic stresses can be compressional or tensional; tensional stresses correspond to regions of high potential energy and positive lithospheric geoid (Coblentz and Sandiford, 1994), suggesting that the lithosphere is in a favorable state for rupture (paths B, B′, and C). We note

that a positive geoid anomaly is obtained when the mantle lithosphere is thinned considerably more than the crust.

MODEL FOR REMOVAL OF MANTLE LITHOSPHERE DURING LATE-STAGE RIFTING

Several factors contribute to uplift during rifting, and the combined effect of phase transitions (path B′, Fig. 3), crustal thickening by magmatic underplating (path C, Fig. 3), and mantle lithosphere that has thinned more than the crust (path B, Fig. 3) will produce (relative) uplift and a positive geoid anomaly favorable for rupture. According to the isostatic calculations discussed here, excess thinning of mantle lithosphere with respect to the crust is very effective in causing uplift and a positive geoid anomaly. The traditional models (McKenzie, 1978) assumed that the mantle lithosphere is expected to thin approximately relatively similar amounts as the crust during rifting, but larger portions of
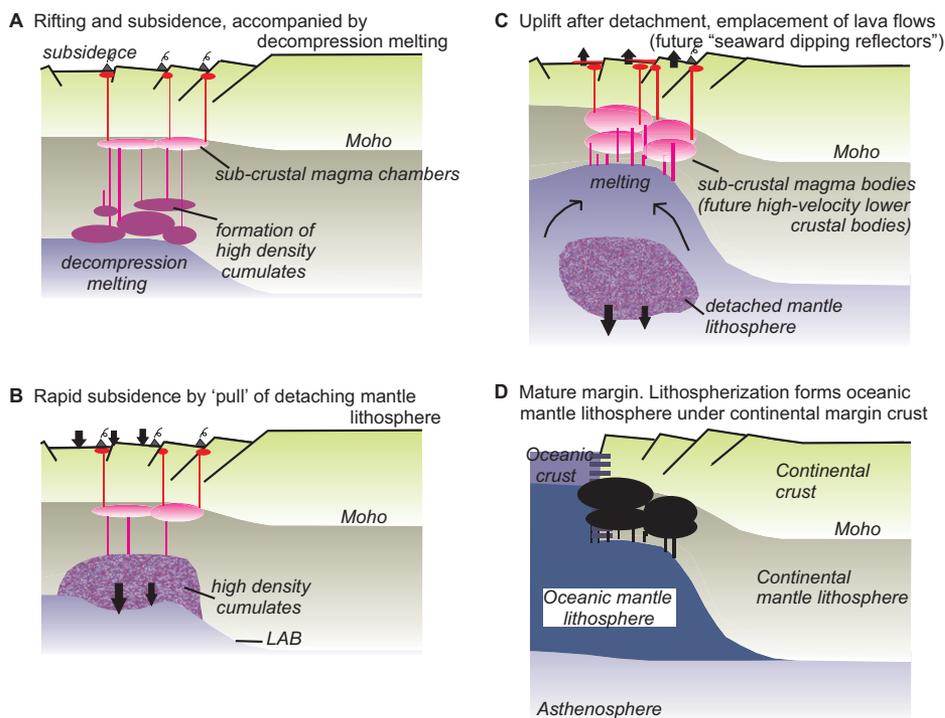

Figure 4. Conceptual model of rifted margin formation. (A) Decompression melting of upwelling asthenosphere accompanies lithosphere thinning during continental rifting. Magmatic differentiation in the lithosphere results in the formation of high-density cumulates. (B) The high-density cumulates destabilize the mantle lithosphere. This results in extra subsidence of the rifted area during detachment. LAB—lithosphere-asthenosphere boundary. (C) After detachment, the surface is uplifted while melting continues, followed by continental rupture. Sub-Moho intrusions are future fast seismic wave velocity lower crustal bodies, lava flows are emplaced at the surface. At magma-poor margins there are no (or few) magmatic eruptions at this time. (D) Following continental breakup, lithospherization of upwelled asthenosphere below the margin occurs.

mantle lithosphere can be lost during rifting by the formation of an instability at the lithosphere-asthenosphere boundary below the rift margin (Sleep, 2007), or by detachment (Fig. 4). Gravitational instabilities (downwellings) may grow by lateral feeding of mantle lithosphere into the drip, which removes mantle from the continental lithosphere. The result is a mantle lithosphere that has thinned more than the crust at the time of continental breakup.

Detachment of mantle lithosphere may follow the formation of high-density magmatic cumulates during the rift phase. Impregnation by substantial volumes of asthenospheric melts has been documented for the extending continental lithospheric mantle of the Jurassic Ligurian Tethys Ocean (Piccardo et al., 2009). The lithospheric mantle may evolve similarly in other rifts. Asthenospheric basanite magmas, generated by decompression melting of rising asthenosphere, infiltrate the continental mantle during the late synrift phase, and undergo continued fractional crystallization during ascent. The denser igneous material is trapped in the continental mantle lithosphere, forming igneous cumulates, while the evolved lighter magmas rise toward shallower cooler layers. Such a high-pressure fractionation model is consistent with experimental petrology (Irving and Green, 2008) and natural lherzolite xenolith-bearing evolved phonolitic magmas within extensional settings, such as the Veste Heldburg (Cenozoic Heldburg dike swarm, Germany). The trapped melts form high-density bodies, and the mantle lithosphere is rheologically modified and weakened, facilitating detachment or removal of large mantle blocks along mantle lithosphere shear zones.

Gravitationally unstable mantle lithosphere will detach and be replaced by warmer asthenosphere, resulting in surface uplift and generation of mid-oceanic ridge basalt–like (MORB) magmas (Meyer et al., 2009a, 2009b). Detachment will occur above the high-density cumulates in the lower mantle lithosphere, and below the region where the density is reduced by phase changes during the advanced stages of rifting. The density effect of phase transitions is mostly pronounced in the uppermost part of the mantle lithosphere during advanced stages of rifting (Simon and Podladchikov, 2008), and detachment will occur between these layers of opposite direction of buoyancy. Pre-detachment rift-related magmas such as found in the East African Rift have a steep rare earth element (REE) pattern (Fig. 5). All continental rift-related magmas are light REE enriched, and this fractionation of the REEs reflects significant high-pressure partial melting in the garnet stability field. In contrast, continental breakup melts such as the seaward-dipping reflector sequences
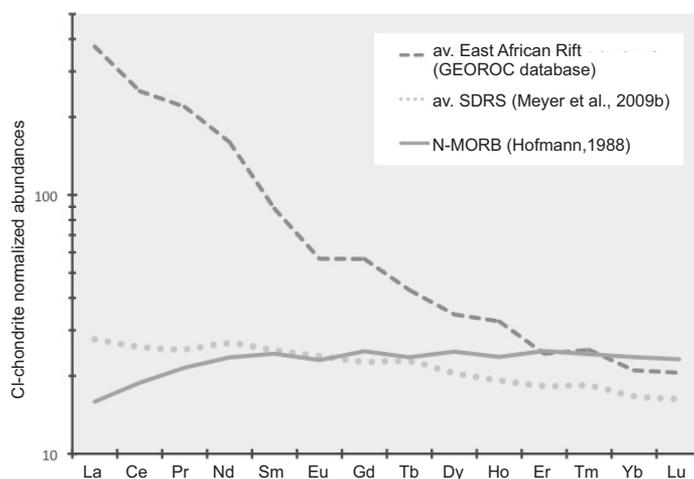

Figure 5. Average (av.) C1-chondrite normalized rare earth element (REE) abundances in melts from a typical rift system (East African Rift), the rift-drift transition at a volcanic rifted margin (seaward-dipping reflector sequence [SDRS] from the Vøring margin), and normal mid-oceanic ridge basalt (N-MORB) illustrate the strongly light REE– to heavy REE–enriched pattern of the rift magmas pointing to garnet as a residual phase in the melting source and the flat REE patterns of the SDRS and the N-MORB due to shallow melting in the mantle. Data sources: C1-chondrite—Palme and O'Neill (2004); average East African Rift system (average inductively coupled plasma mass spectrometry and instrumental neutron activation analysis data from East African Rift)—GEOROC website data set (http://georoc.mpch-mainz.gwdg.de/georoc/webseite/Links.htm); N-MORB—Hofmann (1988); SDRS average—Meyer et al. (2009b).

found on magma-dominated margins (Menzies et al., 2002, and references therein) are subaerial magmas with MORB-like REE enrichment patterns (Fig. 5), illustrating melting of a shallow asthenosphere at the rift to drift transition.

In the model for continental rupture proposed here (Fig. 4), a major difference between magma-starved and magma-dominated margins is the volume of magma that intrudes crustal levels or eventually erupts, and the conceptual model therefore applies to both margin end members. The structural difference between these margin types was described in Reston (2009) and Menzies et al. (2002), and is not discussed here. During extension, the lithosphere is thinned in continental rifts, and upward flow of asthenosphere below the rift results in decompression melting. Differentiation of magma forms high-density cumulates in the mantle lithosphere, while lower density magma rises to shallower levels, ponds in subcrustal magma chambers, and may erupt. The continental mantle is rheologically altered by the melt infiltration, weakened and affected by thermochemical or mechanical erosion. Following detachment of the high-density continental mantle, rapid sur-

face uplift occurs, and the resulting tensional force will assist continental rupture. Melting of upwelling asthenosphere below the remaining continental lithosphere forms oceanic crust. At magma-dominated margins large volumes erupt as basalt flows.

Removal of mantle lithosphere during the late synrift phase by detachment or development of lithospheric downwellings will appear in subsidence curves as extra thinning of the mantle lithosphere; this is depth-dependent thinning of the lithosphere. Depth-dependent thinning is lithosphere thinning where the mantle part has been thinned more than the crust; it has been inferred on many margins (Kusznir and Karner, 2007), supporting the hypothesis that loss of mantle lithosphere is a normal process during rifting.

When the continental mantle lithosphere is removed during the final stages of rifting, it is replaced by asthenosphere. After breakup, the margins cool, and lithospherization of asthenosphere takes place. The process of lithospherization involves cooling of the asthenosphere such that it becomes part of the tectonic plate, analogous to formation of oceanic lithosphere near

mid-ocean ridges. This is accompanied by subsidence of the margin. This newly formed lithosphere from depleted asthenosphere is similar in composition to oceanic mantle lithosphere, and underlies the outermost parts of the continental margin crust (Fig. 4).

CONCLUSIONS

Uplift of margins prior to breakup is typical, and an expected process accompanying continental breakup. It results from several factors, including phase transitions, dynamic uplift, and removal of mantle lithosphere. Removal of mantle lithosphere is most effective in producing uplift or reduced subsidence in combination with phase transitions, and we suggest that mantle lithosphere removal is a common process accompanying rupture. This finding is supported by geochemical data that indicate MORB-like REE enrichment patterns resulting from shallow asthenospheric melting, and observations of depth-dependent thinning. The positive geoid anomaly and increase in tensional forces as a result of this uplift are expected to assist breakup. After breakup, new oceanic mantle lithosphere is formed below the continental margin, and normal subsidence resumes.

REFERENCES CITED

Braun, J., and Beaumont, C., 1989, A physical explanation of the relation between flank uplifts and the breakup unconformity at rifted continental margins: Geology, v. 17, p. 760–764, doi:10.1130/0091-7613(1989)017<0760:APEOTR>2.3.CO;2.

Buck, W.R., 2006, The role of magma in the development of the Afro-Arabian rift system, in Yirgu, G., et al., eds., The Afar volcanic province within the East African Rift System: Geological Society of London Special Publication 259, p. 43–54, doi:10.1144/GSL.SP.2006.259.01.05.

Campbell, I.H., 2005, Large igneous provinces and the mantle plume hypothesis: Elements, v. 1, p. 265–269, doi:10.2113/gselements.1.5.265.

Chazot, G., Menzies, M.A., and Baker, J., 1998, Pre-, syn- and post-rift volcanism on the south-western margins of the Arabian plate, in Purser, B., and Bosence, D., eds., Sedimentation and tectonics in rift basins: Red Sea–Gulf of Aden case: London, Chapman and Hall, p. 50–55.

Coblentz, D., and Sandiford, M., 1994, Tectonic stresses in the African plate: Constraints on the ambient lithospheric stress state: Geology, v. 22, p. 831–834, doi:10.1130/0091-7613(1994)022<0831:TSITAP>2.3.CO;2.

Coblentz, D., and Stüwe, K., 2002, A review of using the f_c-f_l diagram to evaluate continental deformation, in Stein, S., and Freymueller, J.T., eds., Plate boundary zones: American Geophysical Union Geodynamics Series Volume 30, p. 283–294, doi:10.1029/GD030.

Coblentz, D., Chase, C.G., Karlstrom, K.E., and van Wijk, J., 2011, Topography, the geoid, and compensation mechanisms for the southern Rocky Mountains: Geo-

chemistry Geophysics Geosystems, v. 12, Q04002, doi:10.1029/2010GC003459.

Conrad, C.P., and Gurnis, M., 2003, Seismic tomography, surface uplift, and the breakup of Gondwanaland: Integrating mantle convection backwards in time: Geochemistry Geophysics Geosystems, v. 4, 1031, doi:10.1029/2001GC000299.

Dam, G., Larsen, M., and Sonderholm, M., 1998, Sedimentary response to mantle plumes: Implications for Paleocene onshore successions, West and East Greenland: Geology, v. 26, p. 207–210, doi:10.1130/0091-7613(1998)026<0207:SRTMPI>2.3.CO;2.

Dugda, M., Nyblade, A., and Julia, J., 2007, Thin lithosphere beneath the Ethiopian Plateau revealed by a joint inversion of Rayleigh wave group velocities and receiver functions: Journal of Geophysical Research, v. 112, B08305, doi:10.1029/2006JB004918.

Elkins-Tanton, L.T., 2005, Continental magmatism caused by lithospheric delamination, in Foulger, G.R., et al., eds., Plates, plumes, and paradigms: Geological Society of America Special Paper 388, p. 449–461, doi:10.1130/2005.2388(27).

Falvey, D.A., and Mutter, J.C., 1981, Regional plate tectonics and the evolution of Australia's passive continental margins: BMR Journal of Australian Geology and Geophysics, v. 6, p. 1–29.

Gladczenko, T.P., Hinz, K., Eldholm, O., Meyer, H., Neben, S., and Skogseid, J., 1997, South Atlantic volcanic margins: Geological Society of London Journal, v. 154, p. 465–470, doi:10.1144/gsjgs.154.3.0465.

Green, P.F., Thomson, K., and Hudson, J.D., 2001, Recognition of tectonic events in undeformed regions: Contrasting results from the Midland Platform and East Midland Shelf, central England: Geological Society of London Journal, v. 158, p. 59–73, doi:10.1144/jgs.158.1.59.

Gurnis, M., Müller, R.D., and Moresi, L., 1998, Dynamics of Cretaceous vertical motion of Australia and the Australian-Antarctic Discordance: Science, v. 279, p. 1499–1504, doi:10.1126/science.279.5356.1499.

Haxby, W.F., and Turcotte, D.L., 1978, Isostatic geoid anomalies: Journal of Geophysical Research, v. 83, p. 5473–5478, doi:10.1029/JB083iB11p05473.

Hjelstuen, B.O., Eldholm, O., and Skogseid, J., 1999, Cenozoic evolution of the northern Vøring margin: Geological Society of America Bulletin, v. 111, p. 1792–1807, doi:10.1130/0016-7606(1999)111<1792:CEOTNV>2.3.CO;2.

Hofmann, A.W., 1988, Chemical differentiation of the Earth: the relationship between mantle, continental crust, and oceanic crust: Earth and Planetary Science Letters, v. 90, p. 297–314, doi:10.1016/0012-821X(88)90132-X.

Huismans, R., and Beaumont, C., 2011, Depth-dependent extension, two-stage breakup and cratonic underplating at rifted margins: Nature, v. 473, p. 74–78, doi:10.1038/nature09988.

Irving, A.J., and Green, D.H., 2008, Phase relationships of hydrous alkalic magmas at high pressures: Production of nepheline hawaiitic to mugearitic liquids by amphibole-dominated fractional crystallization within the lithospheric mantle: Journal of Petrology, v. 49, p. 741–756, doi:10.1093/petrology/egm088.

Karato, S., and Wu, P., 1993, Rheology of the upper mantle: A synthesis: Science, v. 260, p. 771–778, doi:10.1126/science.260.5109.771.

Keen, C.E., and Dehler, S.A., 1997, Extensional styles and gravity anomalies at rifted continental margins: Some North Atlantic examples: Tectonics, v. 16, p. 744–754, doi:10.1029/97TC01765.

Kooi, H., Cloetingh, S., and Burrus, J., 1992, Lithospheric necking and regional isostasy at extensional basins 1. Subsidence and gravity modeling with an application to the Gulf of Lions Margin (SE Spain): Journal of Geophysical Research, v. 97, p. 17,553–17,571, doi:10.1029/92JB01377.

Kusznir, N.J., and Karner, G.D., 2007, Continental lithospheric thinning and breakup in response to upwelling divergent mantle flow: Application to the Woodlark, Newfoundland and Iberia margins, in Karner, G.D., et al., eds., Imaging, mapping and modeling continental lithosphere extension and breakup: Geological Society of London Special Publication 282, p. 389–419, doi:10.1144/SP282.16.

Larsen, L.M., Fitton, J.G., and Saunders, A.M., 1999, Composition of volcanic rocks from the Southeast Greenland margin, Leg 163: Major and trace element geochemistry, in Larsen, H.C., et al., eds., Proceedings of the Ocean Drilling Program, Scientific results, Volume 163: College Station, Texas, Ocean Drilling Program, p. 63–75, doi:10.2973/odp.proc.sr.163.109.1999.

Lin, A.T., Watts, A.B., and Hesselbo, S.P., 2003, Cenozoic stratigraphy and subsidence history of the South China Sea margin in the Taiwan region: Basin Research, v. 15, p. 453–478, doi:10.1046/j.1365-2117.2003.00215.x.

Lithgow-Bertelloni, C., and Silver, P.G., 1998, Dynamic topography, plate driving forces and the African superswell: Nature, v. 395, p. 269–272, doi:10.1038/26212.

Maclennan, J., and Lovell, B., 2002, Control of regional sea level by surface uplift and subsidence caused by magmatic underplating of Earth's crust: Geology, v. 30, p. 675–678, doi:10.1130/0091-7613(2002)030<0675:CORSLB>2.0.CO;2.

Martinsen, O.J., Boen, F., Charnock, M.A., Mangerud, G., and Nottvedt, A., 1999, Cenozoic development of the Norwegian margin 60–64°N: Sequences and sedimentary response to variable basin physiography and tectonic setting, in Fleet, A.J., and Boldy, S.A.R., eds., Petroleum geology of northwest Europe: Proceedings of the 5th Conference, v. 5: London, Geological Society of London, p. 293–304.

McKenzie, D., 1978, Some remarks on the development of sedimentary basins: Earth and Planetary Science Letters, v. 40, p. 25–32, doi:10.1016/0012-821X(78)90071-7.

Menzies, M.A., Klemperer, S.L., Ebinger, C.J., and Baker, J., 2002, Characteristics of volcanic rifted margins, in Menzies, M.A., et al., eds., Volcanic rifted margins: Geological Society of America Special Paper 362, p. 1–14, doi:10.1130/0-8137-2362-0.1.

Meyer, R., van Wijk, J., and Gernigon, L., 2007, The North Atlantic igneous province: A review of models for its formation, in Foulger, G.R., and Jurdy, D.M., eds., Plates plumes and planetary processes: Geological Society of America Special Paper 430, p. 525–552, doi:10.1130/2007.2430(26).

Meyer, R., Nicoll, G.R., Hertogen, J., Troll, V.R., Ellam, R.M., and Emeleus, C.H., 2009a, Trace element and isotope constraints on crustal anatexis by upwelling mantle melts in the North Atlantic Igneous Province: An example from the Isle of Rum, NW Scotland: Geological Magazine, v. 146, p. 382–399, doi:10.1017/S0016756809006244.

Meyer, R., Hertogen, J., Pedersen, R.-B., Viereck-Götte, L., and Abratis, M., 2009b, Interaction of mantle derived melts with crust during the emplacement of the Vøring Plateau, N.E. Atlantic: Marine Geology, v. 261, p. 3–16, doi:10.1016/j.margeo.2009.02.007.

Mihut, D., and Müller, R.D., 1998, Volcanic margin formation and Mesozoic rift propagators in the Cuvier Abyssal Plain off Western Australia: Journal of Geophysical Research, v. 103, p. 27,135–27,149, doi:10.1029/97JB02672.

Moresi, L., and Gurnis, M., 1996, Constraints on the lateral strength of slabs from three-dimensional dynamic flow models: Earth and Planetary Science Letters, v. 138, p. 15–28, doi:10.1016/0012-821X(95)00221-W.

Moucha, R., Forte, A.M., Rowley, D.B., Mitrovica, J.X., Simmons, N.A., and Grand, S.P., 2009, Deep mantle forces and the uplift of the Colorado Plateau: Geophysical Research Letters, v. 36, L19310, doi:10.1029/2009GL039778.

Palme, H., and O'Neill, H.S., 2004, Cosmochemical estimates of mantle composition, in Holland, H.D., and Turrekian, K.K., eds., Treatise on geochemistry, Volume 2: Amsterdam, Netherlands, Elsevier, p. 1–38, doi:10.1016/B0-08-043751-6/02177-0.

Péron-Pinvidic, G., and Manatschal, G., 2009, The final rifting and evolution at deep magma-poor margins from Iberia-Newfoundland: A new point of view: International Journal of Earth Sciences, v. 98, p. 1581–1597, doi:10.1007/s00531-008-0337-9.

Piccardo, G.B., Vannucci, R., and Guarnieri, L., 2009, Evolution of the lithospheric mantle in an extensional setting: Insights from ophiolitic peridotites: Lithosphere, v. 1, p. 81–87, doi:10.1130/L30.1.

Reston, T., 2009, The structure, evolution and symmetry of the magma-poor rifted margins of the North and Central Atlantic: A synthesis: Tectonophysics, v. 468, p. 6–27, doi:10.1016/j.tecto.2008.09.002.

Sandiford, M., and Coblentz, D., 1994, Plate-scale potential-energy distributions and the fragmentation of ageing plates: Earth and Planetary Science Letters, v. 126, p. 143–159, doi:10.1016/0012-821X(94)90247-X.

Sandiford, M., and Powell, R., 1990, Some isostatic and thermal consequences of the vertical strain geometry in convergent orogens: Earth and Planetary Science Letters, v. 98, p. 154–165, doi:10.1016/0012-821X(90)90056-4.

Saunders, A.D., Fitton, J.G., Kerr, A.C., Norry, M.J., and Kent, R.W., 1997, The North Atlantic Igneous Province, in Mahoney, T.J., and Coffin, M.F., eds., Large igneous provinces: Continental, oceanic and planetary flood volcanism: American Geophysical Union Geophysical Monograph 100, p. 45–93, doi:10.1029/GM100p0045.

Schärer, U., Girardeau, J., Cornen, G., and Boillot, G., 2000, 138–121 Ma asthenospheric magmatism prior to continental break-up in the North Atlantic and geodynamic implications: Earth and Planetary Science Letters, v. 181, p. 555–572, doi:10.1016/S0012-821X(00)00220-X.

Simon, N.S.C., and Podladchikov, Y.Y., 2008, The effect of mantle composition on density in the extending lithosphere: Earth and Planetary Science Letters, v. 272, p. 148–157, doi:10.1016/j.epsl.2008.04.027.

Skogseid, J., and Eldholm, O., 1989, Vøring Plateau continental margin: Seismic interpretation, stratigraphy, and vertical movements, in Eldholm, O., et al., eds., Proceedings of the Ocean Drilling Program, Scientific results, Volume 104: College Station, Texas, Ocean Drilling Program, p. 993–1030, doi:10.2973/odp.proc.sr.104.151.1989.

Skogseid, J., Pedersen, T., and Larsen, V.B., 1992, Vøring Basin: Subsidence and tectonic evolution, in Larsen, R.M., et al., eds., Structural and tectonic modeling and its application to petroleum geology: Norwegian Petroleum Society Special Publication 1, p. 55–82.

Sleep, N., 2007, Edge-modulated stagnant-lid convection and volcanic passive margins: Geochemistry Geophysics Geosystems, v. 8, Q12004, doi:10.1029/2007GC001672.

Song, T., and Cawood, P.A., 2000, Structural styles in the Perth Basin associated with the Mesozoic breakup of greater India and Australia: Tectonophysics, v. 317, p. 55–72, doi:10.1016/S0040-1951(99)00273-5.

van Hunen, J., and Zhong, S., 2003, New insight in the Hawaiian plume swell dynamics from scaling laws: Geophysical Research Letters, v. 30, 1785, doi:10.1029/2003GL017646.

van Wijk, J., van Hunen, J., and Goes, S., 2008, Small-scale convection during continental rifting: Evidence from the Rio Grande rift: Geology, v. 36, p. 575–578, doi:10.1130/G24691A.1.

Veevers, J.J., 2000, Change of tectono-stratigraphic regime in the Australian plate during the 99 Ma (mid-Cretaceous) and 43 Ma (mid-Eocene) swerves of the Pacific: Geology, v. 28, p. 47–50, doi:10.1130/0091-7613(2000)28<47:COTRIT>2.0.CO;2.

White, R.S., and McKenzie, D., 1989, Magmatism at rift zones: The generation of volcanic continental margins and flood basalts: Journal of Geophysical Research, v. 94, p. 7685–7729, doi:10.1029/JB094iB06p07685.

White, R.S., Spence, G.D., Fowler, S.R., McKenzie, D.P., Westbrook, G.K., and Bowen, A.N., 1987, Magmatism at rifted continental margins: Nature, v. 330, p. 439–444, doi:10.1038/330439a0.

Wilson, R.C.L., Manatschal, G., and Wise, S., 2001, Rifting along nonvolcanic passive margins: Stratigraphic and seismic evidence from the Mesozoic successions of the Alps and western Iberia, in Wilson, R.C.L., et al., eds., Non-volcanic rifting of continental margins: A comparison of evidence from land and sea: Geological Society of London Special Publication 187, p. 429–452, doi:10.1144/GSL.SP.2001.187.01.21.

Withjack, M.O., Schlische, R.W., and Olsen, P.E., 1998, Diachronous rifting, drifting, and inversion on the passive margin of central eastern North America: An analog for other passive margins: American Association of Petroleum Geologists Bulletin, v. 82, p. 817–835.

Xie, X., Müller, R.D., Li, S., Gong, Z., and Steinberger, B., 2006, Origin of anomalous subsidence along the Northern South China Sea margin and its relationship to dynamic topography: Marine and Petroleum Geology, v. 23, p. 745–765, doi:10.1016/j.marpetgeo.2006.03.004.

Yirgu, G., Ebinger, C.J., and Maguire, P.K.H., 2006, The Afar volcanic province within the East African Rift System: Introduction, in Yirgu, G., et al., eds., The Afar volcanic province within the East African Rift system: Geological Society of London Special Publication 259, p. 1–6, doi:10.1144/GSL.SP.2006.259.01.01.

Zhong, S., Zuber, M.T., Moresi, L., and Gurnis, M., 2000, Role of temperature-dependent viscosity and surface plates in spherical shell models of mantle convection: Journal of Geophysical Research, v. 105, p. 11,063–11,082, doi:10.1029/2000JB900003.